  Bull. Chem. Soc. Jpn., **66**, 3289–3299(1993)

Formation of the Oxanickelacyclopentene Complex from Nickel(0), Carbon Dioxide, and Alkyne. An *ab initio* MO/SD-CI Study[#]

Shigeyoshi SAKAKI,* Kazuya MINE, Daisaku TAGUCHI, and Toru ARAI
Department of Applied Chemistry, Faculty of Engineering, Kumamoto University, Kurokami, Kumamoto 860
(Received May 13, 1993)

An *ab initio* MO/SD-CI study was carried out on the formation reaction of oxanickelacyclopentene, (H_3P)–$\overline{\text{Ni–CH=CH–CO}}$(O) **1**, from $Ni(PH_3)$, CO_2, C_2H_2. Because C_2H_2 coordinates to $Ni(PH_3)$ more strongly than does CO_2 by ca. 11 kcal mol^{-1} at the SD-CI level, coordination of C_2H_2 to $Ni(PH_3)$ takes place first. The resultant $Ni(PH_3)(C_2H_2)$ reacts with CO_2 to yield **1** with no activation barrier and a significant *exo*-thermicity of 68 kcal mol^{-1} at the HF level, but a moderate barrier of 30 kcal mol^{-1} and *exo*-thermicity of 17 kcal mol^{-1} at the SD-CI level. **1** takes a three-coordinate T-shaped structure, due to the low-spin d^8 electron configuration of Ni(II). $Ni(PH_3)$ stabilizes the transition state through a charge-transfer interaction from the occupied d orbital of Ni to the unoccupied π^* orbitals of CO_2 and C_2H_2. The electron re-distribution during the reaction is discussed, based on orbital mixing among the d orbital of Ni and the π and π^* orbitals of C_2H_2 and CO_2.

The chemical utilization of CO_2 for the synthesis of various organic compounds is an attractive research subject, as has been recently reviewed.[1] Of particular interest are the transition metal-catalyzed coupling reactions of CO_2 with such unsaturated hydrocarbons as dienes,[2—4] trienes,[5] and alkynes,[6—10] since chemically useful 2-pyrone derivatives and α,β-unsaturated acids are produced. In these reactions, oxametallacyclopentene and oxametallacyclopentane have been postulated as being key intermediates, as shown in Eqs. 1 and 2.

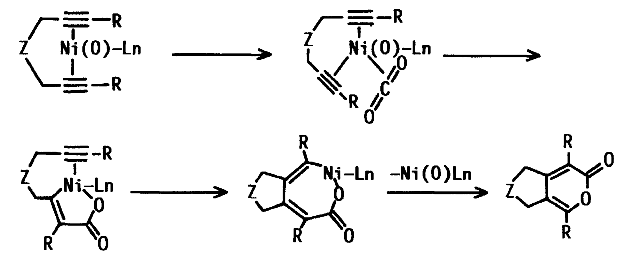

(1)

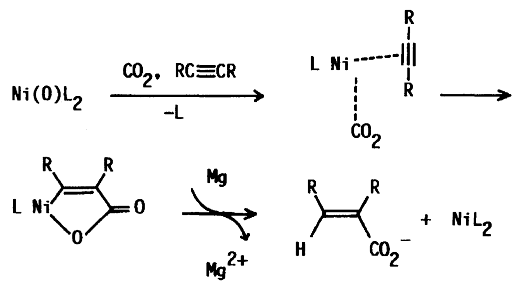

(2)

Similar metallacycle complexes have been considered as key intermediates in transition-metal catalyzed mutual coupling of alkenes or alkynes.[11] As is well-known, the mutual coupling reaction of alkenes or alkynes in a (2s+2s) geometry is symmetry forbidden. However, the transition metal complex weakens the symmetry-forbidden nature and allows the coupling reaction to proceed easily, as has been theoretically explained by Hoffmann and collaborators.[12] In the coupling reaction between carbon dioxide and alkyne, the situation is slightly different from the mutual coupling reactions, as follows: The symmetry is lower than in the mutual coupling of alkenes or alkynes, and HOMO of carbon dioxide is not a π orbital, but a non-bonding π orbital. We can thus expect that the symmetry-forbidden nature is weaker in this coupling reaction than in the mutual coupling reaction. Nevertheless, the transition metal complex is indispensable for this coupling reaction, as is well-known expermentally,[2—10] and is clearly shown in the present work. From both viewpoints of CO_2 fixation and transition metal catalysis, therefore, it is of fundamental importance to theoretically investigate the coupling reaction between CO_2 and alkynes and to clarify the role that the transition metal complex plays in this coupling reaction. So far, several theoretical studies have been carried out on Ni(0)–CO_2 complexes[13,14] in which the coordinate bonding nature and coordinating structure of CO_2 have been mainly discussed. However, only a few theoretical studies have been reported concerning the coupling reaction between CO_2 and alkene.[14a,14c]

In the present work, the formation of oxanickelacyclopentene, $(H_3P)\overline{\text{Ni–CH=CH–CO}}$(O) **1**, from $Ni(PH_3)$, CO_2, and C_2H_2 (Eq. 3) was investigated using the *ab initio* MO/SD-CI method. This reaction is considered to be a key step of a nickel(0)-catalyzed 2-pyrone synthesis from CO_2 and alkyne.[3—10] The aims of the present work were (1) to estimate the activation energy and the energy of the reaction, (2) to show how the geometry and electron distribution change during the reaction, (3) to present a theoretical explanation for those changes, and (4) to provide a detailed understanding of the origin of the Ni(0) catalysis in this coupling reaction. It was also our intention to provide the first quantitative

#This paper is dedicated to the late Professor Hiroshi Kato.

~ semiquantitative picture of this coupling reaction.

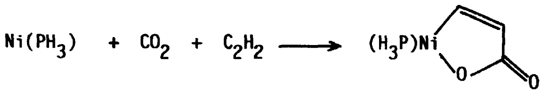

(3)

Computational Details

Models of Reaction System and Their Geometries. Although both four- and three-coordinate Ni(0) complexes have been reported, Ni(0) complexes of alkene, alkyne, CO_2, and their analogues have been known to be mostly of the three-coordinate type. For instance, $Ni(PR_3)(C_2H_4)_2$, $Ni(PH_3)(C_2H_2)(C_2H_4)$, and $Ni(PR_3)(C_2H_2)_2$ have been reported in NMR studies (Scheme 1).[15] It is thus not unlikely to suppose that C_2H_2 and CO_2 coordinate to $Ni(PH_3)$ to yield $Ni(PH_3)(C_2H_2)(CO_2)$. This three-coordinate system is adopted here as a reaction model. Actually, the $Ni(COD)_2$–PR_3 equimolar system catalyzes a 2-pyrone synthesis.[8,9a] Of course, the authors do not rule out the possibility that the formation of oxanickelacyclopentene proceeds on the four-coordinate Ni(0) complex, $Ni(L)_2(C_2H_2)(CO_2)$ ($L=PR_3$ etc.), since the Ni(0) complex with chelate phosphine, bipyridine, or 2—4 equiv of monodentate phosphine efficiently catalyzes 2-pyrone formation.[3—7,9,10] In this study, three coordinate reaction system was first investigated in detail; the four-coordinate reaction system was then compared with the three-coordinate system.

All of the optimizations were carried out at the Hartree–Fock (HF) level using the energy-gradient method in which the geometry of PH_3 was fixed to the experimental sturcture of a free PH_3 molecule.[16] The geometry of the reaction system of $Ni(PH_3)(C_2H_2)(CO_2)$ was optimized at a fixed θ ($=\angle X_1NiX_2$) angle, where X_1 and X_2 are the center of the C≡C triple bond of C_2H_2 and that of the C=O double bond of CO_2, respectively (Scheme 2); the angle was rather arbitrarily taken to be 130°, 120°, 110°, 100°, 95°, 90°, 85°, 80°, 75°, and 70° as a reaction coordinate. The geometry of $Ni(PH_3)_2(C_2H_2)(CO_2)$ was optimized at only $\theta=75°$ (note that this system is too large to carry out a detailed examination).

***ab initio* MO/SD-CI Calculations.** Spin-restricted *ab initio* MO and limited SD-CI calculations were carried out using the Gaussian 86[17] and MELD[18] programs. Three kinds of basis sets (BS-I, BS-II, and BS-III) were employed. In the BS-I set used for geometry optimization, MIDI-3 sets[19] and the (4s)/[2s] set[20] were adopted for C, O, and H respectively. The valence electrons of P and Ni were represented by (3s 3p)/[2s 2p] and (3s 2p 5d)/[2s 2p 2d] split-valence basis functions, respectively, while the core electrons of P (up to 2p) and those of Ni (up to 3p) were replaced by effective core potentials (ECP) of Hay and Wadt.[21a,21b] In the BS-II set used for SD-CI calculations of $Ni(PH_3)(C_2H_2)$, $Ni(PH_3)(CO_2)$, $Ni(PH_3)(C_2H_2)(CO_2)$, and $(H_3P)\overline{Ni\text{–}CH\text{=}CH\text{–}CO}(O)$, MIDI-4 sets were employed for all of the ligand atoms.[19] For Ni, Huzinaga's (13s 7p 5d) primitive set proposed for the $^3D(d^9s)$ state of Ni[19] was augmented with a diffuse d primitive ($\zeta=0.10$) and three p primitives whose exponents were taken to be the same as the three most diffuse s primitives of Ni. The resultant (13s 10p 6d) primitive set was contracted to a [5s 4p 3d] split-valence basis function. In the BS-III set used for SD-CI calculations of $Ni(PH_3)_2(C_2H_2)$, $Ni(PH_3)_2(C_2H_2)(CO_2)$, and $(H_3P)_2\overline{Ni\text{–}CH\text{=}CH\text{–}CO}(O)$, ECPs[21b,21c] were employed for the core electrons of P (up to 2p) and Ni (up to 2p) in order to reduce the computation time (note the large size and low symmetry of $Ni(PH_3)_2(C_2H_2)(CO_2)$). For Ni, a triple-ζ basis set (5s 5p 5d)/[3s 3p 3d][21c] was adopted to represent the valence electrons, including 3s and 3p electrons. For P, the same basis set as in the BS-I set was adopted to represent the valence 3s and 3p electrons. For the other atoms, MIDI-4 sets were employed.

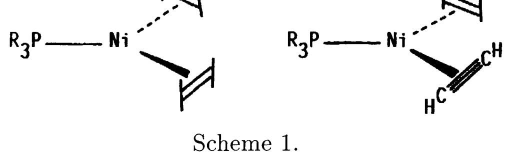

Scheme 1.

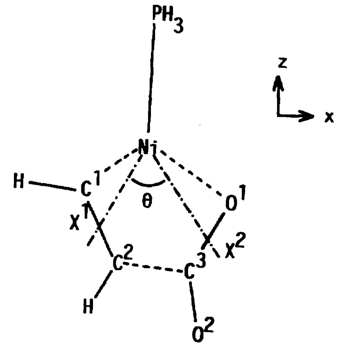

Scheme 2.

Limited SD-CI calculations were carried out with a single Hartree–Fock (HF) configuration as a reference, where all of the core orbitals were excluded from the active space and virtual orbitals were transformed to K-orbitals[22] in order to improve the convergence of CI. All possible spin-adapted configuration functions were screened by using second-order Rayleigh–Schrödinger perturbation theory[23] to reduce the number of configuration functions on which variational SD-CI calculations were performed. The energy threshold adopted in the perturbation selection was 50 μhartree. The SD-excited configurations remaining after the perturbation selection included over 90% of the estimated SD correlation energy. The results of limited SD-CI calculations were corrected by estimating the correlation energy arising from the discarded SD excited configuration functions. A correction for the higher order CI expansions was then made[24] in order to yield E_t(est full-CI). All of the discussion is based on the E_t(est full-CI) value.

As shown in Table 1, the coefficient for the HF reference is about 0.91 in the single-reference (SR) SD-CI calculation. To ascertain the reliability of the SR SD-CI calculations, multi-reference (MR) SD-CI calculations were carried out on two important geometries (θ=95° and 80°, see above for θ), where the HF and K-orbitals were used for the occupied and virtual orbitals, respectively. Although the sum of the squares of the CI coefficients for the reference configurations is not sufficiently large, even in the MR SD-CI calculations, the energy difference (ΔE) between two structures changes only slightly upon going to the MR SD-CI calculation from the SR SD-CI calculation (see Table 1). Thus, the results of the SR SD-CI calculations seem to be reliable in at least estimating the energy change of this reaction.

Results and Discussion

Geometries and Coordinate Bonds of Ni(PH_3)(C_2H_2) and Ni(PH_3)(CO_2). Prior to investigating the coupling reaction, we need to examine the geometries and coordinate bonds of the reactants. As shown in Fig. 1, the optimized structure of Ni(PH_3)(C_2H_2) is bent (**2b**). The linear structure **2a** was optimized under the assumption of the C_s symmetry. Although **2b** is 2.4 kcal mol^{-1} more stable than **2a** at the HF level, **2a** is 2.0 kcal mol^{-1} more stable than **2b** at the SD-CI level. Furthermore, **2a** converts to **2b** with only a small barrier at both the HF and SD-CI levels. These results indicate that the coordination structure of Ni(PH_3)(C_2H_2) is flexible and that C_2H_2 easily changes its coordination site. The C_2H_2 part is significantly distorted in **2a** and **2b**; the C–C distance is about 0.2 Å longer than in the free C_2H_2 molecule (Fig. 1), and the CCH angle is 138°. This distorted structure suggests that a strong back-bonding interaction is involved in Ni(PH_3)(C_2H_2). Consistent with this suggestion, a significant charge-transfer (0.94 e) occurs from Ni(PH_3) to C_2H_2. The C_2H_2 part of Ni(PH_3)$_2$(C_2H_2) **4** is also significantly distorted; its geometry agrees well with the experimental structure.[25] A discussion concerning **4** is omitted here because it has previously been investigated in detail.[26]

In the case of Ni(PH_3)(CO_2), an only bent structure **3** is obtained from an optimization. The pseudo-linear structure[27] was calculated to be less stable than **3** by ca. 6 kcal mol^{-1} at the SD-CI level. In **3**, the C=O bond coordinating to Ni lengthens to 1.33 Å from its equilibrium value (1.16 Å) and the OCO angle is 135°. This distorted structure agrees well with the experimental structure of CO_2 in Ni(PCy_3)$_2$(η^2-CO_2).[28]

The coordinate bonds of CO_2 and C_2H_2 are compared by considering the following assumption:[29]

$$\underset{\mathbf{3}}{\mathrm{Ni(PH_3)(CO_2)}} + \mathrm{C_2H_2} \rightleftarrows \underset{\mathbf{2a}}{\mathrm{Ni(PH_3)(C_2H_2)}} + \mathrm{CO_2}. \quad (4)$$

The difference in the total energies between the right- and left-hand sides ($E_{\mathrm{right}} - E_{\mathrm{left}}$) was calculated to be +0.3 kcal mol^{-1} at the HF level, but −10.7 kcal mol^{-1} at the SD-CI level. We now briefly discuss the reason that **2a** is more stable than **3**. Since the HF calculation of Ni(PH_3) failed, an energy decomposition analysis could not be carried out on **2a** and **3**; a detailed discussion concerning the coordinate bond of **2a** and **3** is therefore difficult. However, a qualitative understanding of the relative stabilities of **2a** and **3** is possible from previous theoretical studies of Ni(PH_3)$_2$(CO_2) and Ni(PH_3)$_2$(C_2H_4).[13a,13c] The electrostatic (ES) interaction in Ni(PH_3)$_2$(C_2H_4) is stronger than that in Ni(PH_3)$_2$(CO_2), since two negatively charged C atoms intereact with the positively charged Ni atom in the former, but one negatively charged O and one positively charged C atom interact with Ni in the latter. The same situation exists in Ni(PH_3)(C_2H_2) and Ni(PH_3)(CO_2) (note that Ni is positively charged in these neutral molecules). In these complexes, CO_2 and C_2H_2 significantly distort, forming a strong back-bonding interaction which is important in these complexes. Back bonding seems not to be very different in these complexes, considering that the Mulliken populations of CO_2 and C_2H_2 increase to a similar extent. However, the distortion energy (34.0 kcal mol^{-1}) of CO_2 is slightly larger than that (30.3 kcal mol^{-1}) of C_2H_2. Although information concerning the other interactions (donating interaction, dispersion interaction etc.) is ambiguous, the greater ES interaction and smaller distortion energy at least favor the coordination of C_2H_2 more than that of CO_2.

From these results, a coherent picture concerning the formation of the Ni(PH_3)(C_2H_2)(CO_2) reaction system might emerge as follows: First, the coordination of acetylene to Ni(PH_3) takes place to form linear Ni(PH_3)(C_2H_2) **2a**; secondly, **2a** offers a coordinating site to CO_2 by changing to the best structure **2b**, and then CO_2 interacts with (or coordinates to) **2b** to yield the Ni(PH_3)(C_2H_2)(CO_2) reaction system.

The C_2H_2–CO_2 Coupling Reaction on Ni(PH_3). The changes in the geometry and energy during the coupling reaction are shown in Figs. 2, 3, and 4 as a function of θ.[30a] The **5** (θ=120°) and **6**(θ=110°) exhibit a similar stabilization energy, and both are only 4 kcal mol^{-1} more stable than Ni(PH_3)(C_2H_2) **2a**+CO_2 at the SD-CI level (a correction of the basis set super position error (BSSE) by the counterpoise method decreases the stabilization energy of **6** to ca. 1 kcal mol^{-1}). The reaction system becomes less stable upon both an increase or decrease in θ.[30b] In **6**, the distance between C^3 of CO_2 and C^2 of C_2H_2 is 3.01 Å. This means that the C^2–C^3 bond between CO_2 and C_2H_2 is not formed at all. Consistent with this suggestion, the geometry

Table 1. Comparison of Single Reference SD-CI and Multi Reference SD-CI Calculations[a)]

Reference function		ΣC_i^2 [b)]	Perturbation selection[c)]		ΔE[d)]
Numbers	Configuration[e)]		Kept	Discard	kcal mol^{-1}
1	HF-configuration	0.831	0.863	0.076	20.2
2[f)]	$+(d\pi+\phi_4)^2 \rightarrow (d\pi-\phi_4)^2$	0.832	0.860	0.076	20.3
4[g)]	$+(\pi_\perp)^2 \rightarrow (\pi_\perp^*)^2$ of C_2H_2 $+(\pi_\perp)^2 \rightarrow (\pi_\perp^*)^2$ of CO_2	0.838	0.783	0.087	20.7
5	$+(d\pi+\phi_4)^1 \rightarrow (d\pi-\phi_4)^1$	0.841	0.784	0.087	19.3

a) MR SD-CI calculations were carried out for θ=95° and 80°. b) Sum of the square of the CI coefficients in the reference space (θ=80°). c) At θ=80°. d) [E(est. full-CI) at θ=80°]−[E(est. full-CI) at θ=95°]. e) The bonding interaction is represented by "+" and the anti-bonding interaction is represented by "−". f) See Fig. 7 for ϕ_4. g) These $\pi_\perp$ and $\pi_\perp^*$ are the perpendicular to the molecular plane.

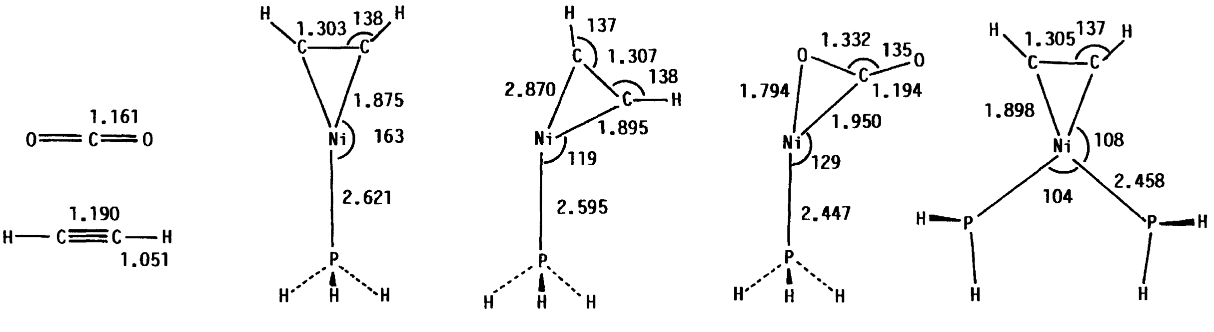

2a **2b** **3** **4**

Fig. 1. Optimized structures of the reactants. Bond length in Å and bond angle in degree.

of the C_2H_2 part hardly changes from that of **2b**. Interestingly, the geometry of the CO_2 part is far from it in Ni(PH_3)(CO_2); for instance, the C–O bond approaching Ni(0) slightly lengthens to 1.18 Å and the OCO angle is 172°, indicating that only a slight distortion takes place in the CO_2 part. Considering this small stabilization energy and slightly distorted geometry of CO_2, it can be reasonably concluded that **5** and **6** can be regarded not as being the usual charge-transfer-type complex, but as a van der Waals complex between Ni(PH_3)(C_2H_2) and CO_2. This result is consistent with a picture in which the coupling reaction proceeds via the approach of CO_2 to Ni(PH_3)(C_2H_2).

Here, we should mention a previous theoretical proposal in which the coupling reaction between CO_2 and alkene proceeds via the approach of alkene to Ni(NH_3)$_2$(CO_2).[14a,14c)] In that work the coordinate structures of Ni(NH_3)$_2$(CO_2) and Ni(NH_3)$_2$(C_2H_4) were investigated using the CAS-SCF method; the slide movement of CO_2 from the η^2-side-on coordination to the η^1-O-coordination was calculated to occur more easily than a similar movement of C_2H_4. From this result, the approach of C_2H_4 to Ni(NH_3)$_2$(CO_2) has been proposed. In our calculations, on the other hand, the initial structure **5** can be seen to be consistent with a picture in which CO_2 approaches Ni(PH_3)(C_2H_2). This picture is considered not to change upon the introduction of electron correlation, because the HF calculation tends to overestimate the binding energy of CO_2 more than that of C_2H_2 (vide supra). The difference between the previous proposal and ours would result from the co-existing ligand. In the model examined previously, two molecules of NH_3 coordinate to Ni, in which the approach of a substrate to Ni is difficult. In Ni(NH_3)$_2$(CO_2), therefore, the slide movement of CO_2 is necessary in order to allow a substrate to approach Ni. Thus, a picture in which C_2H_4 approaches Ni(NH_3)$_2$(CO_2) seems reasonable, because the slide movement in Ni(NH_3)$_2$(CO_2) occurs more easily than in Ni(NH_3)$_2$(C_2H_4). In our reaction system, one PH_3 coordinates to Ni, which facilitates the approach of a substrate by the bending of Ni(PH_3)L (L=C_2H_2 or CO_2); therefore, the slide movement is not necessary for the coupling reaction. This means that the reaction course would not be influenced by the ease of the slide movement, but due to the relative stabilities of Ni(PH_3)(C_2H_2) and Ni(PH_3)(CO_2). Thus, a picture in which the coupling reaction proceeds via the approach of CO_2 to Ni(PH_3)(C_2H_2) seems to be reasonable in the reaction system examined here, because Ni(PH_3)(C_2H_2) is more stable than Ni(PH_3)(CO_2).

As the θ value decreases (i.e., as CO_2 approaches C_2H_2), the C–C bond of the C_2H_2 part slightly lengthens, which is not surprising, since its C–C bond is already considerably long in **2a** and **2b**. In the CO_2 part, on the other hand, the C=O bond coordinating to Ni be-

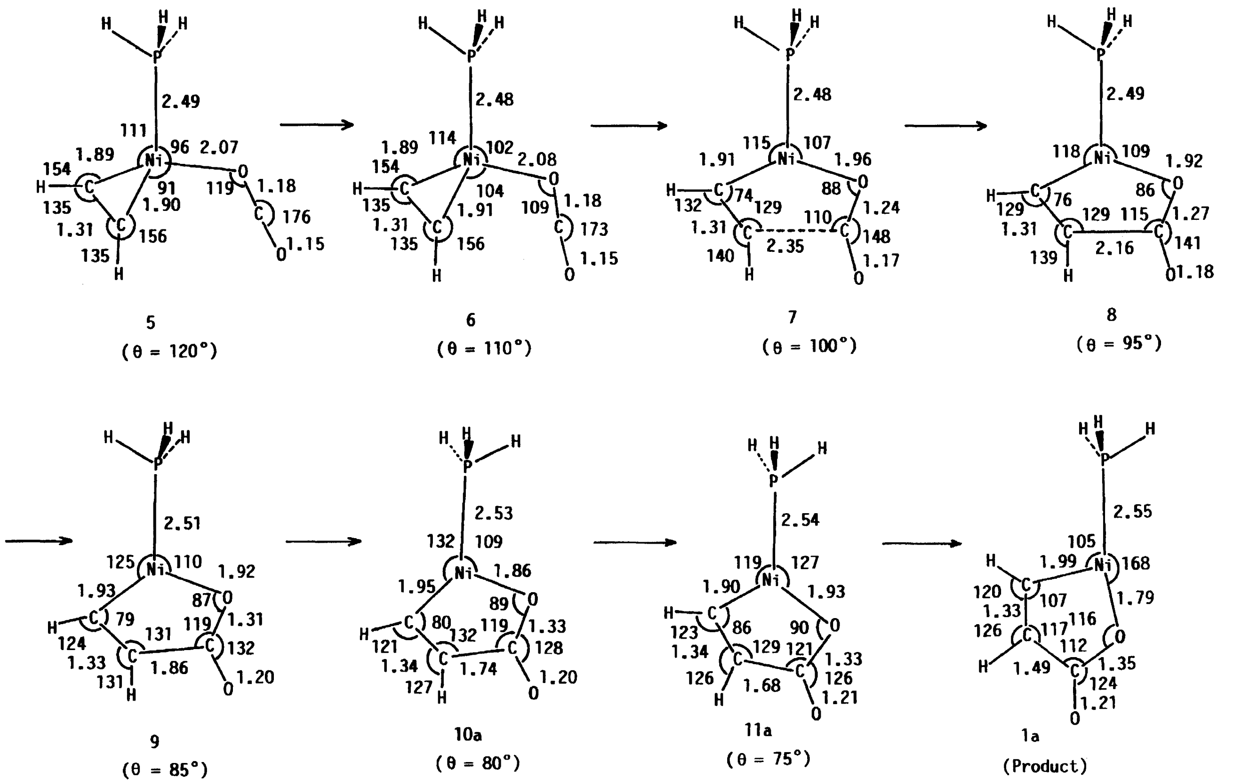

Fig. 2. Geometry changes during the coupling reaction between CO_2 and C_2H_2 along the reaction path 1. Bond length in Å and bond angel in degree. Geometries at $\theta=90°$ and 70° are omitted to save the space.

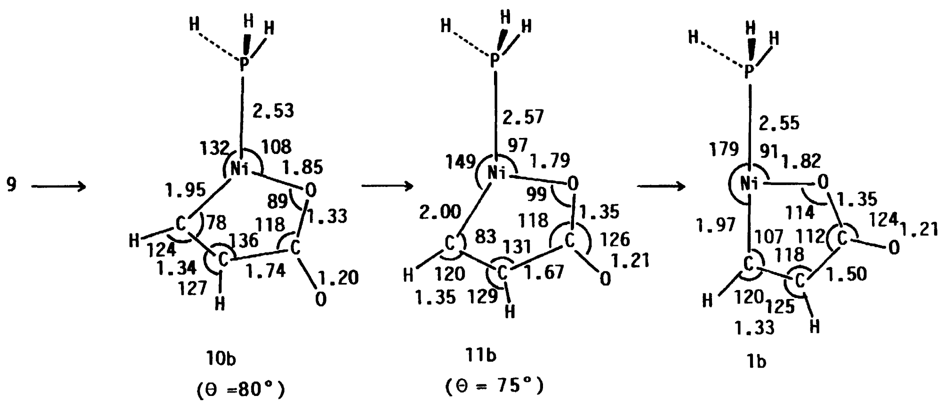

Fig. 3. Geometry changes during the coupling reaction between CO_2 and C_2H_2 along the reaction path 2.[a)] Bond length in Å and bond angle in degree. a) Geometries after **8** are given with the geometry at 70° omitted for brevity.

comes long and the OCO angle becomes small. These changes in the CO_2 part seem to be reasonable, since the CO_2 part is only slightly distorted at **5** and **6**.

The important result to be recognized is that the reaction path separates into two parts around the transition state (TS) ($\theta\approx80°$), and that there are two isomers, **1a** and **1b**, in the product, $(H_3P)\overline{Ni{-}CH{=}CH{-}C}O(O)$, as shown in Figs. 2 and 3; although in **1a**, PH_3 lies at the trans-position to the oxygen atom, in **1b** it exists at the trans-position to the carbon atom. Here the reaction course leading to **1a** is called path 1, and the reaction course leading to **1b** is path 2. Both reactions along paths 1 and 2 proceed with a slight activation barrier, but significant *exo*-thermicity (68 kcal mol^{-1} for **1a** and 69 kcal mol^{-1} for **1b**) at the HF level (Fig. 4), where the *exo*-thermicity is defined as the energy difference between **1** and **2a**+CO_2, and the activation barrier is the energy difference between TS and **6**. However, the situation completely changes upon going to the SD-CI level from the HF level. The reaction along path 1 proceeds with a moderate activation barrier of 30 kcal mol^{-1} and an *exo*-thermicity of 16 kcal mol^{-1}.[31)] The reaction along path 2 occurs with a slightly higher activation barrier of 40 kcal mol^{-1} and a slightly smaller *exo*-thermicity of 12.6 kcal mol^{-1}.

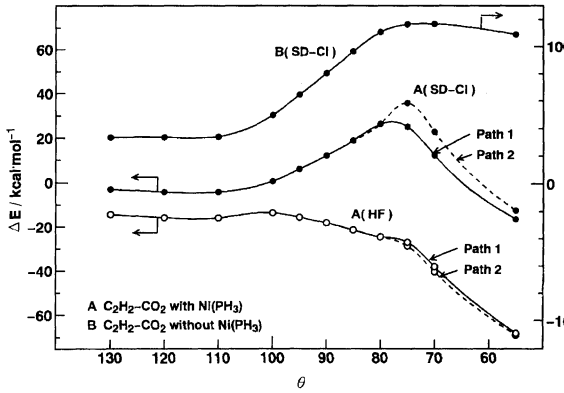

Fig. 4. Energy changes[a)] during the coupling reaction between CO_2 and C_2H_2. a) Standard (energy 0) is taken for the infinite separation between CO_2 and $Ni(PH_3)(C_2H_2)$.

The TS is found at around **10a** ($\theta \approx 80°$) in path 1 and around **11b** ($\theta \approx 75°$) in path 2. The TS exhibits the following geometrical features: (1) the C^2–C^3 distance between CO_2 and C_2H_2 is 1.74 Å in **10a** and 1.67 Å in **11b**, suggesting that the C^2–C^3 bond is not completely formed at the TS; (2) the C^1NiO^1 angle is 120° in **10a** and 114° in **11b**, somewhat greater than in the products; and (3) the C–C bond distance of the C_2H_2 part and the C–O bond distance of the CO_2 part are close to those in the products. Here, it should be mentioned that the difference in the activation barrier between paths 1 and 2 is much greater than the energy difference between **1a** and **1b** (discussed below).

We now inspect the difference between products **1a** and **1b**. Both **1a** and **1b** take the T-shaped structure, due to the low-spin d^8 electron configuration of Ni(II), as has been clearly explained by Hoffmann et al.[32)] **1a** is calculated to be only 4.0 kcal mol^{-1} more stable than **1b** at the SD-CI level. The relative stabilities of **1a** and **1b** are easily interpreted in terms of the trans-influence of PH_3. In **1a**, the trans-position of the carbon atom is empty, while the trans-position of the oxygen atom is occupied by PH_3. In **1b**, the trans-position of the carbon atom is occupied by PH_3, while the trans-position of the oxygen atom is empty. Because the carbon atom exhibits a stronger trans-influence than does the oxygen atom, **1a** is more favorable than **1b**. However, the difference in the energy between the two structures is unexpectedly small (vide supra). This would result from the steric repulsion between the CH group and PH_3; in **1a**, the PNiC angle is 105°, considerably larger than 90°, which is probably due to a steric repulsion between the CH group and the PH_3 ligand. In **1b**, on the other hand, both the PNiO and ONiC angles are about 90°. Thus, although the trans influence of PH_3 would favor **1a**, the steric repulsion would favor **1b**, leading to the small energy difference between **1a** and **1b**.

Since C_2H_2 insertion into the Ni–C^1 bond must occur in the next step (see Eq. 1), **1a** should convert to **1b**. The inter-coversion between them was roughly examined, as shown in Fig. 5.[33)] The activation barrier of this inter-conversion was estimated to be ca. 6 kcal mol^{-1} at the SD-CI level. Thus, the inter-conversion between **1a** and **1b** occurs more easily than does C_2H_2–CO_2 coupling reaction from **5** to **1a**.

In the absence of $Ni(PH_3)$, the approach of CO_2 to C_2H_2 causes a significant destabilization in the energy (Fig. 4), as expected, where the geometries of CO_2 and C_2H_2 are taken to be the same as those in Fig. 2, and only the $Ni(PH_3)$ part is removed from the reaction system. Thus, $Ni(PH_3)$ is indispensable for the C_2H_2–CO_2 coupling reaction.

Electron Re-distribution during the Coupling Reaction. Electron re-distribution along the reaction path 1 is mainly discussed here. First, we examine the C_2H_2–CO_2 coupling reaction in the absence of $Ni(PH_3)$. As shown in Fig. 6, although the electron population of C_2H_2 decreases, the electron population of CO_2 increases, as CO_2 approaches C_2H_2. These changes suggest that the charge-transfer from C_2H_2 to CO_2 becomes strong as the reaction proceeds. The atomic populations also exhibit interesting changes: (1) the O^1 atomic population increases significantly, much more than the O^2 and C^3 atomic populations (see Scheme 2 for C^1, C^2 etc.); (2) the C^1 atomic population decreases during the early stage of the reaction, but slightly increases during the late stage of the reaction; (3) the C^2 atomic population decreases during the late stage of the reaction.

This electron re-distribution is easily explained based on the orbital mixing rule.[34)] In the C_2H_2–CO_2 system, the π and π^* orbitals of C_2H_2 interact with π, π^*, and non-bonding π ($n\pi$) orbitals of CO_2 to yield ϕ_1—ϕ_5,

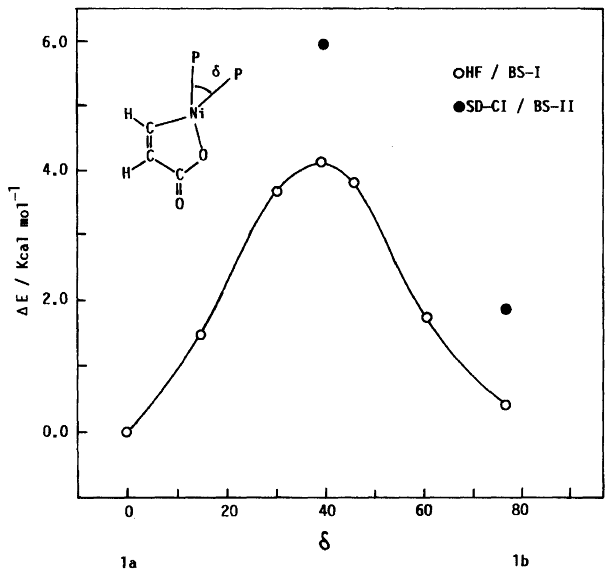

Fig. 5. Energy changes in the inter-conversion between **1a** and **1b**.[a)] a) See Figs. 2 and 3 for **1a** and **1b**. **1a** is taken as a standard (energy 0).

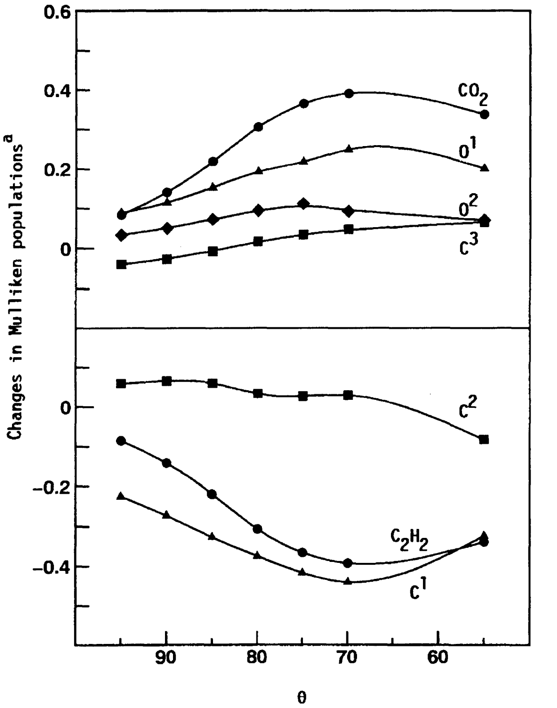

Fig. 6. Mulliken population changes[a)] during the C_2H_2–CO_2 coupling reaction without $Ni(PH_3)$. a) Mulliken population changes are given here for an important range of the reaction from $\theta=95°$ to the product. A positive value means an increase in population and a negative value means a decrease. See Scheme 2 for C^1, C^2 etc.

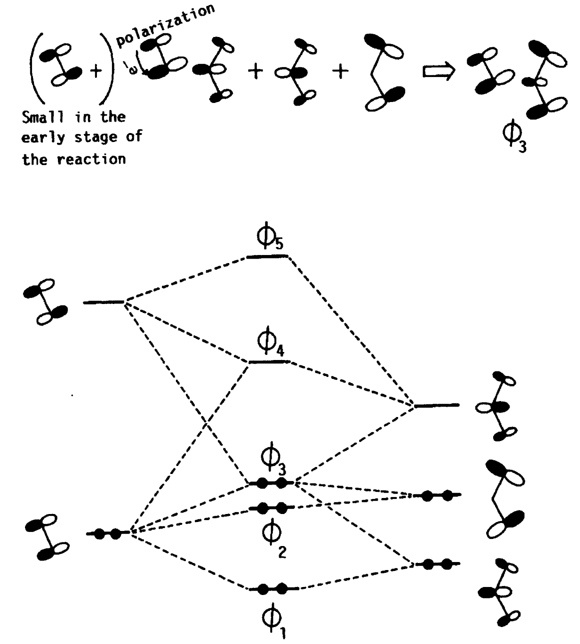

Fig. 7. Orbital interaction diagram in the C_2H_2–CO_2 coupling reactions without $Ni(PH_3)$.

as shown in Fig. 7. The HOMO (ϕ_3) involves an anti-bonding overlap between the π orbitals of C_2H_2 and CO_2, into which the π^* orbital of CO_2 mixes in a bonding way. However, the $n\pi$ orbital of CO_2 only slightly mixes in an anti-bonding way. In HOMO, therefore, the p_π contribution is considerably enhanced on the O^1 atom, moderately on the O^2 atom, but reduced on the C^3 atom, which leads to a significant increase in the O^1 atomic population and a moderate increase in the O^2 atomic population. Although the orbital mixing predicts a slight decrease in the C^3 atomic population, the C^3 atomic population slightly increases (Fig. 6), probably due to a strong charge transfer from C_2H_2 to the π^* orbital of CO_2. Similar electron re-distribution and orbital mixings of the CO_2 part have been reported in an *ab initio* MO study of the CO_2 insertion into the Cu(I)–H bond.[35)]

In the C_2H_2 part, the C^1 atomic population decreases during the early stage of the reaction, as expected, but unexpectedly slightly increases during the late stage of the reaction. This increase is explained by considering the orbital mixing of the π^* orbital of C_2H_2 into the ϕ_3 orbital in a bonding way with the π orbital of CO_2. During the early stage of the reaction, this orbital mixing is weak, since the overlap between the π^* orbital of C_2H_2 and the π orbital of CO_2 is small. During the late stage of the reaction, however, this mixing becomes important, due to an increase in the overlap, to enhance the p_π contribution of the C^1 atom to the ϕ_3 (see Fig. 7) and to increase the C^1 atomic population.

In the presence of $Ni(PH_3)$, the electron population of CO_2 increases and the electron population of C_2H_2 decreases to a lesser extent than in the reaction system without $Ni(PH_3)$, as shown in Fig. 8. The Ni atomic population and the Ni d orbital population exhibits complicated changes: Both decrease during the early stage of the reaction, reach a minimum around the TS, and then increase during the late stage of the reaction, while the s and p orbital populations of Ni change only slightly during the reaction (they are omitted in Fig. 8 for brevity). Interesting changes are also observed in the CO_2 and C_2H_2 parts: (1) as the reaction proceeds, the O^1 atomic population significantly increases and the O^2 atomic population moderately increases, as in the reaction system without $Ni(PH_3)$; (2) the C^1 atomic population slightly increases, the C^2 atomic population significantly decreases, and the C^3 atomic population slightly decreases, unlike in the reaction system without $Ni(PH_3)$. The electron re-distribution in the reaction system with $Ni(PH_3)$ is expected to reflect the catalysis of $Ni(PH_3)$. When $Ni(PH_3)$ is involved in the reaction system, the d orbitals of Ni can participate in the orbital mixing. Here, we discuss the reaction system, separating it into two parts, $Ni(PH_3)$ and C_2H_2–CO_2. As shown in Fig. 9, the $d_{x^2-z^2}$ orbital of Ni is the HOMO of $Ni(PH_3)$ and the d_{xz} orbital of Ni lies at a lower energy than the $d_{x^2-z^2}$ orbital. Of five ϕ_1—ϕ_5 orbitals in the C_2H_2–CO_2 part, the ϕ_3 and ϕ_4 orbitals mainly interact with the Ni d_{xz} and $d_{x^2-z^2}$ orbitals. The

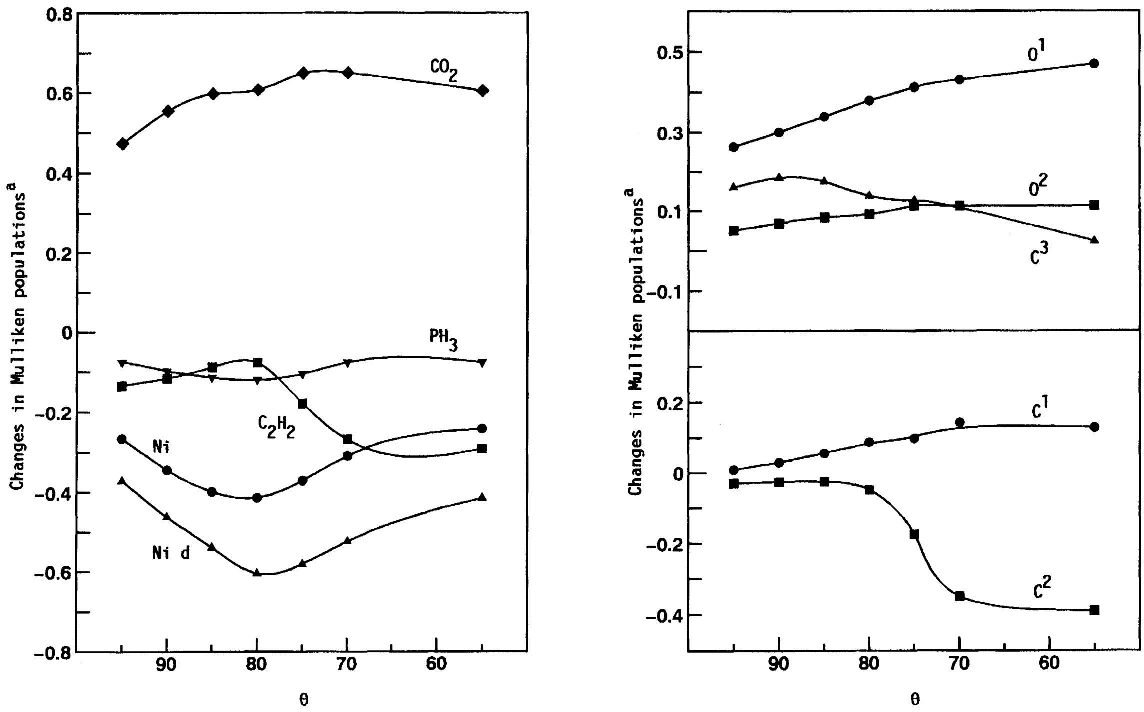

Fig. 8. Mulliken population changes[a)] during the C_2H_2–CO_2 coupling reaction with $Ni(PH_3)$. a) See footnote a) of Fig. 6.

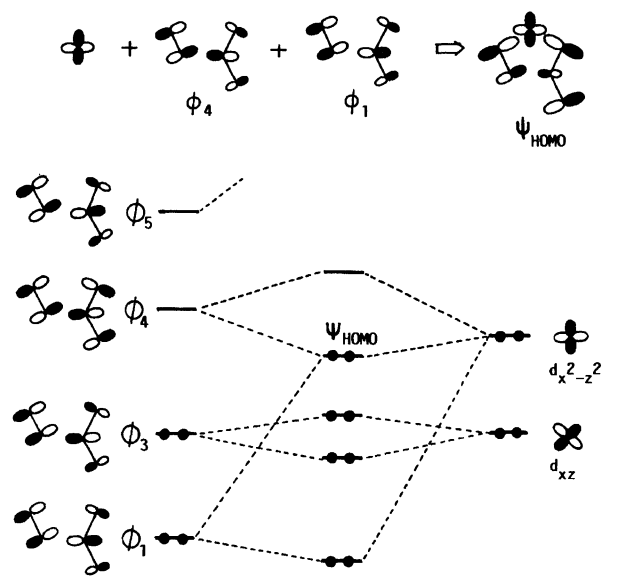

Fig. 9. Orbital interaction diagram in the C_2H_2–CO_2 coupling reaction with $Ni(PH_3)$.[a)] a) The ϕ_2 is omitted here for brevity.

d_{xz} orbital interacts with the ϕ_3 orbital of the C_2H_2–CO_2 part, which yields a four-electron destabilizing interaction, since both the d_{xz} and ϕ_3 orbitals are doubly occupied. On the other hand, the $d_{x^2-z^2}$ orbital can form a strong charge-transfer interaction to the ϕ_4 orbital to yield the HOMO (Ψ_{HOMO}), because of a large overlap between the $d_{x^2-z^2}$ and ϕ_4 orbitals (see Fig. 9). This charge-transfer interaction significantly decreases the $d_{x^2-z^2}$ orbital population, stabilizes the reaction system, and enhances the C^2–C^3 bonding interaction between C_2H_2 and CO_2 (note that the ϕ_4 orbital includes the C^2–C^3 bonding interaction between CO_2 and C_2H_2). Into this Ψ_{HOMO}, the ϕ_1 orbital mixes so as to weaken the C^2–C^3 bonding interaction, because the ϕ_1 orbital lies at a lower energy than does the ϕ_4 orbital. As shown in Fig. 9, this anti-bonding mixing of ϕ_1 enhances the p_π contribution on C^1, O^1, and O^2 atoms, but reduces the p_π contribution on C^2 and C^3 atoms. In the $Ni(PH_3)(C_2H_2)(CO_2)$ system, these orbital mixings work with the orbital mixings in the ϕ_3 orbital of the C_2H_2–CO_2 part discussed above. Consequently, the C^2 and C^3 atomic populations considerably decrease, the C^1 and O^2 atomic populations moderately increase, and the O^1 atomic population considerably increases. The reliability of these orbital mixings would be justified by the contour map of the HOMO of $Ni(PH_3)(C_2H_2)(CO_2)$ (at $\theta=75°$). As shown in Fig. 10, the HOMO exhibits the following features: (1) the HOMO mainly consists of the π^* orbital of C_2H_2 and the deformed π^* orbital of CO_2; (2) the contribution of the Ni $d_{x^2-z^2}$ orbital is small, suggesting that considerable charge-transfer occurs from $Ni(PH_3)$ to the C_2H_2–CO_2 part; (3) the C^2–C^3 bonding interaction clearly exists between C_2H_2 and CO_2; (4) in the CO_2 part, the p_π contribution of the C^3 atom is considerably reduced, but the p_π contributions of the O^1 and O^2 atoms are enhanced; and (5) in the C_2H_2 part, the C^1 p_π contribution is larger than the C^2 p_π contribution. All of these features certainly agree well with the prediction from the orbital mixing

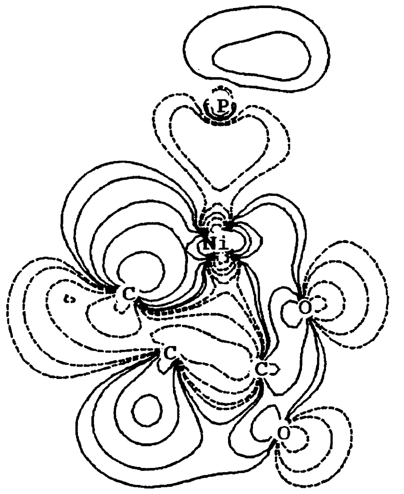

Fig. 10. Contour map of HOMO of $Ni(PH_3)(C_2H_2)$-(CO_2) at θ=75°. Values; ±0.2, ±0.1, ±0.05, ±0.02, ±0.01.

rule.

In summary, $Ni(PH_3)$ stabilizes the reaction system by a charge-transfer interaction from $Ni(PH_3)$ to C_2H_2–CO_2, which enhances the C–C bond formation between C_2H_2 and CO_2. This implies that the strongly donating ligand facilitates the coupling reaction, since it favors a charge-transfer from Ni to C_2H_2–CO_2. In fact, although PPh_3 is ineffective, electron-donating PCy_3 is effective for a Ni(0)-catalyzed 2-pyrone synthesis.[8,9a)]

Here, we briefly discuss the reason that the d-orbital population of Ni increases during the late stage of the reaction. After TS, the reaction system changes from the C_{3h}-like structure to the T-shaped one. In the C_{3h}-like structure, the d orbital contributes to the coordinate bond to a lesser extent than in the T-shaped one because the rigid C_{3h} structure takes the sp^2 hydridization and the T-shaped product includes the dsp^2-like hybridization (note that the T-shaped complex resembles the square planar complex from the point of view of electronic structure). Thus, the d-orbital contribution increases upon going to the T-shaped product from the TS, which leads to an increase in the d-orbital populaiton after TS.

Comparison of the Four–Coordinate Reaction System, $Ni(PH_3)_2(C_2H_2)(CO_2)$ with the Three-Coordinate Reaction System, $Ni(PH_3)(C_2H_2)$-(CO_2). We now examine the C_2H_2–CO_2 coupling by $Ni(PH_3)_2$. The geometry of $Ni(PH_3)_2(C_2H_2)(CO_2)$ was optimized at θ=75°.[36)] In the optimization, the planar structure was assumed, whereas the tetrahedral-like structure seemed to be reasonable in Ni(0) complexes. When we discuss the geometry and electronic structure around the TS, this assumption seems to be plausible, since Ni is seen to be similar to the d^8 system around the TS, due to the significant charge transfer from the Ni d orbital to π^* orbitals of CO_2 and C_2H_2. As shown in Fig. 11, the Ni–P^2 distance (3.1 Å) trans-positioned

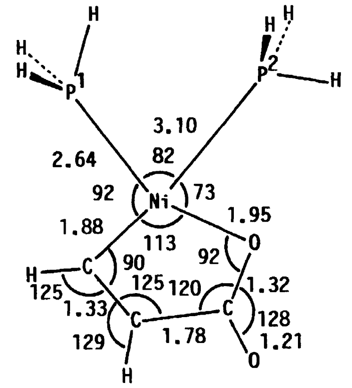

12

Fig. 11. Optimized geometry of $Ni(PH_3)_2(C_2H_2)$-(CO_2) at θ=75°. Bond length in Å and bond angle in degree.

to the C atom is much longer than the usual coordinate bond. Even after considering that the present HF optimization tends to yield a rather long Ni–P distance, as exemplified by the Ni–P^1 distance trans-positioned to the oxygen atom, this Ni–P^2 distance is too long. It is thus reasonably concluded that two molecules of PH_3 are difficult to coordinate to Ni around TS, and that one PH_3 positioned trans to the C atom cannot coordinate to Ni, but only weakly interacts with Ni.

It is also noted here that the C^2–C^3 distance between CO_2 and C_2H_2 in the $Ni(PH_3)_2(C_2H_2)(CO_2)$ system is longer than in the $Ni(PH_3)(C_2H_2)(CO_2)$ system (compare **11a** in Fig. 2 and **12** in Fig. 11). This implies that the four-coordinate reaction system is less favorable for the C–C bond formation between CO_2 and C_2H_2 than the three-coordinate system. The C–C bond formation is accelerated by a charge-transfer from Ni to the ϕ_4 orbital of the C_2H_2–CO_2 part, as discussed above. Because the HOMO of $Ni(PH_3)_2$ is mainly composed of the d_{xz} orbital of Ni, as is well known, it does not overlap well with the ϕ_4 orbital of the C_2H_2–CO_2 part, as shown in Scheme 3. Thus, the four-coordinate reaction system is not favorable for the charge-transfer interaction from Ni to ϕ_4. In the three-coordinate reaction system, on the other hand, considerable charge-transfer occurs from Ni to the C_2H_2–CO_2 part, as discussed above.

The energy change in the $Ni(PH_3)_2(C_2H_2)(CO_2)$ reaction system also reflects the less favorable situation for the C^2–C^3 bond formation. **12** is less stable than

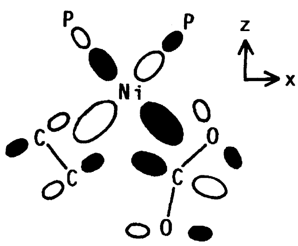

Scheme 3.

$Ni(PH_3)_2(C_2H_2)$ **4**+CO_2 by ca. 35 kcal mol^{-1} at the SD-CI level (BS-III),[38] suggesting that the activation energy of the four-coordinate reaction system is greater than that of the three-coordinate system. Consequently, the four-coordinate reaction system is less favorable for the stabilization of TS and the C–C bond formation between C_2H_2 and CO_2 than the three-coordinate system.

Conclusion

The formation of oxanickelacyclopentene, (R_3P)Ni–CH=CH–CO(O) **1**, from $Ni(PH_3)$, CO_2, and C_2H_2 was investigated with the *ab initio* MO/SD-CI method. The consideration of electron correlation is indispensable for any theoretical investigation of this reaction, since the results at the HF level differ from the results at the SD-CI level, even in a qualitative sense.

C_2H_2 coordinates to $Ni(PH_3)$ more strongly than does CO_2 by ca. 11 kcal mol^{-1} at the SD-CI level. The linear structure **2a** of $Ni(PH_3)(C_2H_2)$ is more stable than its bent form **2b** by only 2 kcal mol^{-1} at the SD-CI level. These results suggest that the coordination of C_2H_2 to $Ni(PH_3)$ takes place first to yield **2a**, which offers a reaction site to CO_2 by changing to the bent form **2b**. CO_2 interacts weakly with **2b** to yield the reaction system of $Ni(PH_3)(C_2H_2)(CO_2)$, on which the C_2H_2–CO_2 coupling reaction proceeds. There are two possible structures in the product **1**: in one (**1a**), PH_3 lies at the trans-position of the O^1 atom; in the other (**1b**), however, PH_3 exists at the trans-position of the C^1 atom. The coupling reaction between $Ni(PH_3)(C_2H_2)$ and CO_2 yields **1a** and **1b** with activation barriers of 30 and 40 kcal mol^{-1}, respectively, and an *exo*-thermicity of 17 and 13 kcal mol^{-1}, respectively, at the SD-CI level. **1a** is about 4 kcal mol^{-1} more stable than **1b**, which is interpreted in terms of the trans-influence of PH_3. An inter-conversion between **1a** and **1b** proceeds with an activation barrier of ca. 6 kcal mol^{-1} at the SD-CI level, less than the barrier of the coupling reaction yielding **1a** from $Ni(PH_3)(C_2H_2)$ and CO_2. The electron re-distribution during the coupling reaction is easily interpreted by considering the orbital mixing rule. From the electron re-distribution and orbital mixing, it is reasonably concluded that the charge-transfer from $Ni(PH_3)$ to the π^* orbitals of C_2H_2 and CO_2 is important to stabilize the TS of this coupling reaction and to enhance the C–C bond formation betwen C_2H_2 and CO_2.

In the C_2H_2–CO_2 coupling by $Ni(PH_3)_2$, two molecules of PH_3 are difficult to coordinate to Ni around TS; although one PH_3 trans-positioned to the O atom can coordiante to Ni, the other PH_3 trans-postioned to the C atom cannot coordiante to Ni, but only weakly interacts with Ni. The C–C bond formation between C_2H_2 and CO_2 is less favorable than in the three coordinate reaction system, due to the unfavorable situation for the charge-transfer from Ni to the C_2H_2–CO_2 part.

In summary, a good catalyst for CO_2 fixation into 2-pyrone derivatives is a low-valent transition metal complex which exhibits a strong Lewis basicity. The use of a donating ligand is also recommended.

One of the authors (SS) is very grateful to the late professor Hiroshi Kato for his generous encouragement since SS started MO studies of transition metal complexes. The authors gratefully acknowledge helpful and stimulating discussions with Professor Tetsuo Tsuda (Kyoto University). All of the calculations were carried out at Institute for Molecular Science (Okazaki, Japan) by using Hitach S-820 and M-680 computers. The authors also acknowledge the Ministry of Education, Culture and Science, for the financial support (Grant-in-Aid No. 04243102).

References

1) For instance: a) S. Inoue and N. Yamazaki, "Organic and Bio-Organic Chemistry of Carbon Dioxide," Kodansha Ltd., Tokyo (1982); b) D. J. Darensbourg and R. A. Kudaroski, *Adv. Organomet. Chem.*, **22**, 129 (1983). c) D. Walther, *Coord. Chem. Rev.*, **79**, 135 (1987). d) A. Behr, *Angew, Chem., Int. Ed. Engl.*, **27**, 661 (1988). e) P. Braunstein, D. Matt, and D. Nobel, *Chem. Rev.*, **88**, 747 (1988). f) A. R. Culter, P. K. Hanna, and J. C. Vites, *Chem. Rev.*, **88**, 1363 (1988).

2) Y. Sasaki, Y. Inoue, and H. Hashimoto, *J. Chem. Soc., Chem. Commun.*, **1976**, 605.

3) A. Behr, R. He, K. -D. Juseak, C. Kruger, and Y. -H. Tsay, *Chem. Ber.*, **119**, 991 (1986), and references are therein.

4) a) H. Hoberg, S. Gross, and A. Milchereit, *Angew. Chem., Int. Ed. Engl.*, **26**, 571 (1987), and references are therein; b) H. Hoberg, Y. Peres, A. Milchereit, and S. Gross, *J. Organomet. Chem.*, **345**, C17 (1988); c) H. Hoberg and D. Barhausen, *J. Organomet. Chem.*, **379**, C7 (1989).

5) A. Behr and U. Kanne, *J. Organomet. Chem.*, **317**, C41 (1986).

6) Y. Inoue, Y. Itoh, H. Kazama, and H. Hashimoto, *Bull. Chem. Soc. Jpn.*, **53**, 3329 (1980).

7) a) G. Burkhart and H. Hoberg, *Angew. Chem., Int. Ed. Engl.*, **21**, 76 (1982); b) H. Hoberg, D. Schaefer, G. Burkhart, C. Kruger, and M. J. Romao, *J. Organomet. Chem.*, **266**, 203 (1984).

8) D. Walther, H. Schonberg, E. Dinjus, and J. Sieler, *J. Organomet. Chem.*, **334**, 377 (1987).

9) a) T. Tsuda, S. Morikawa, R. Sumiya, and T. Saegusa, *J. Org. Chem.*, **53**, 3140 (1988); b) T. Tsuda, S. Morikawa, and T. Saegusa, *J. Chem. Soc., Chem. Commun.*, **1989**, 9; c) T. Tsuda, K. Kunisada, N. Nagahara, S. Morikawa, and T. Saegusa, *Synth. Commun.*, **19**, 1575 (1989); **20**, 313 (1990); d) T. Tsuda, S. Morikawa, N. Hasegawa, and T. Saegusa, *J. Org. Chem.*, **55**, 2978 (1990); e) T. Tsuda, K. Maruta, and Y. Kitaike, *J. Am. Chem. Soc.*, **114**, 1498 (1992).

10) a) E. Dunach, S. Derien, and J. Perichon, *J. Organomet. Chem.*, **364**, C33 (1989); b) S. Derien, J. -C. Clinet, E. Dunach, and J. Perichon, *J. Chem. Soc., Chem.*

Commun., **1991**, 549; c) S. Derien, E. Dunach, and J. Perichon, *J. Am. Chem. Soc.*, **113**, 8447 (1991).

11) For instance: A. Nakamura, *Coord. Chem. Rev.*, **109**, 207 (1991).

12) a) A. Stockis and R. Hoffmann, *J. Am. Chem. Soc.*, **102**, 2952 (1980); b) R. J. McKinney, D. L. Thorn, R. Hoffmann, and A. Stockis, *J. Am. Chem. Soc.*, **103**, 2595 (1981).

13) a) S. Sakaki, K. Kitaura, and K. Morokuma, *Inorg. Chem.*, **21**, 760 (1982); b) S. Sakaki, K. Kitaura, K. Morokuma, and K. Ohkubo, *Inorg, Chem.*, **22**, 104 (1983); c) S. Sakaki, N. Koga, and K. Morokuma, *Inorg. Chem.*, **29**, 3110 (1990).

14) a) A. Dedieu and F. Ingold, *Angew, Chem., Int. Ed. Engl.*, **28**, 1694 (1989); b) C. Jegat, M. Fouassier, M. Tranquille, J. Mascetti, I. Tommasi, M. Aresta, F. Ingold, and A. Dedieu, *Inorg. Chem.*, **32**, 1279 (1993); c) A. Dedieu, C. Bo, and F. Ingold, "Enzyme Model Carboxylation Reduction Reaction, Carbon Dioxide Utilization," NATO ASI Ser. C, Reidle, Dordrecht (1990), p. 23.

15) K. -R. Pörschke, *J. Am. Chem. Soc.*, **111**, 5691 (1989).

16) G. Herzberg, "Molecular Spectra and Molecular Structure," D. Van Nostrand, Co., Princeton, NJ, (1976), Vol. 3, p. 610.

17) M. J. Frisch, J. S. Binkley, H. B. Schlegel, K. Raghavachari, C. F. Melius, R. Martin, J. J. P. Stewart, F. W. Bobrowicz, C. M. Rohlfing, L. R. Kahn, D. J. DeFrees, R. Seeger, R. A. Whiteside, D. J. Fox, E. M. Fluder, and J. A. Pople, "Carnegie–Mellon Quantum Chemistry Publishing Unit," Pittsburgh, PA (1986).

18) E. R. Davidson, L. McMurchie, S. Elbert, S. R. Langhoff, D. Rawlings, and D. Feller, "MELD IMS Computer Center Library, No. 030," Unversity of Washington, Seattle, WA.

19) S. Huzinaga, J. Andzelm, M. Klobukowski, E. Radzio-Andzelm, Y. Sakai, and H. Tatewaki, "Gaussan Basis Sets for Molecular Calculations," Elsevier, Amsterdam (1984).

20) T. H. Dunning and P. J. Hay, "Gaussian Basis Sets for Molecular Calculation," in "Methods of Electronic Structure Theory," ed by H. F. Schaefer, Plenum, New York (1977), p. 1.

21) a) P. J. Hay and W. R. Wadt, *J. Chem. Phys.*, **82**, 270 (1985); b) W. R. Wadt and P. J. Hay, *J. Chem. Phys.*, **82**, 284 (1985); c) P. J. Hay and W. R. Wadt, *J. Chem. Phys.*, **82**, 299 (1985).

22) D. Feller and E. R. Davidson, *J. Chem. Phys.*, **74**, 3997 (1981).

23) S. R. Langhoff and E. R. Davidson, *Int. J. Quantum Chem.*, **8**, 61 (1974).

24) E. R. Davidson and D. W. Silver, *Chem. Phys. Lett.*, **52**, 403 (1977).

25) R. S. Dickson and J. A. Ibers, *J. Organomet, Chem.*, **36**, 191 (1972).

26) K. Kitaura, S. Sakaki, and K. Morokuma, *Inorg. Chem.*, **20**, 2292 (1981).

27) The Ni–P bond was assumed to be collinear to the vertical line from Ni to the C=O bond of CO_2.

28) M. Aresta, C. F. Nobile, V. G. Albano, E. Forni, and M. J. Manassero, *J. Chem. Soc., Chem. Commun.*, **1975**, 636.

29) Because $Ni(PH_3)$ could not be optimized by both the HF/BS-I and SD-CI/BS-II calculations, we could not estimate the binding energies of C_2H_2 and CO_2 to $Ni(PH_3)$.

30) a) Because the oxacyclopentene ring is considered to be highly conjugated, optimization was carried out under assumption of the C_s symmetry, where the xz-plane is taken to be a symmetry plane. b) Because the potential curve regarding θ is very shallow and flat, we did not optimize the minimum.

31) In general, the activation barrier becomes lower upon introducing electron correlation. The present result is reverse to this expectation. There are two possible reasons, at least; the first, the HF description of the free CO_2 is not sufficiently good but rather poor, and the second, the basis set used is not sufficient for the molecule calculated here. Details are not known at the present stage and further investigation is necessary.

32) S. Komiya, T. A. Alblight, R. Hoffmann, and J. K. Kochi, *J. Am. Chem. Soc.*, **98**, 7255 (1976).

33) The δ angle (see Fig. 5) was varied rather arbitrarily, where the geometry of the Ni–CH=CH–CO(O) part and the Ni-P distance were assumed by a linear transit so as to turn smoothly from **1a** to **1b**.

34) a) S. Inagaki and K. Fukui, *Chem. Lett.*, **1974**, 509; b) S. Inagaki, H. Fujimoto, and K. Fukui, *J. Am. Chem. Soc.*, **98**, 4054 (1976).

35) S. Sakaki and K. Ohkubo, *Inorg. Chem.*, **28**, 2583 (1989).

36) Geometry optimization of $Ni(PH_3)_2(C_2H_2)(CO_2)$ requires so long computation time that the geometry optimization was carried out only for θ=75°.

37) This value is not the activation energy, but the activation energy would be higher than this value.

38) It is ambiguous whether **12** is TS or not. If **12** is the TS, the activation barrier is 35 kcal mol^{-1}. If not, the activation barrier is higher than 35 kcal mol^{-1}.